Functional Materials 12, No.2 (2005)

Luminescent properties of Ce^{3+} ions in alkaline earth borophosphates

V.P.Dotsenko, I.V.Berezovskaya, N.P.Efryushina, A.S.Voloshinovskii[*], *C.W.E.van Eijk*[**], *P.Dorenbos*[**], *A.Sidorenko*[**]

A.Bogatsky Physico-Chemical Institute, National Academy of Sciences of Ukraine, Lustdorfskaya doroga 86, 65080 Odessa, Ukraine
[*]I.Franko Lviv State University, Kirilo i Mefodii 8, 79005 Lviv, Ukraine
[**]Delft University of Technology, Mekelweg 15, 2629 JB Delft, The Netherlands

The luminescence properties of Ce^{3+} ions in alkaline earth borophosphates $MBPO_5$ (M = Sr, Ba) have been studied upon excitation in the 3.5–15 eV region. It has been shown that the splitting of the Ce^{3+} 5*d* configuration due to crystal field in $MBPO_5$ (M = Sr, Ba) is relatively large, nevertheless, the lowest 5*d* state of Ce^{3+} is at a relatively high energy due to the high degree of ionicity of the M–O bond. Comparison of the luminescence excitation spectra for $MBPO_5:Ce^{3+}$ (M = Ca, Sr, Ba) indicates that the fundamental absorption band of these host lattices is due to transitions within anionic groups.

Изучены люминесцентные свойства ионов Ce^{3+} в борофосфатах $MBPO_5$ (M = Sr, Ba) при возбуждении в области 3.5–15 эВ. Показано, что расщепление кристаллическим полем 5*d*-конфигурации ионов Ce^{3+} в $MBPO_5$ (M = Sr, Ba) относительно велико, тем не менее, нижнее 5*d* состояние ионов Ce^{3+} характеризуется достаточно большой энергией, что обусловлено высокой степенью ионности связи M–O. Сопоставление спектров возбуждения люминесценции показывает, что полоса фундаментального поглощения $MBPO_5$ обусловлена переходами внутри анионных групп.

The luminescent properties of Eu^{2+} ions in alkaline earth borophosphates of the general formula $MBPO_5$ (M = Ca, Sr, Ba) have been studied by several authors [1–3]. It has been shown that the Eu^{2+}-doped borophosphates are efficient photoluminescent materials. In recent years, materials of $MBPO_5:Eu^{2+}$ (M = Ca, Sr) composition gained a special attention because of possible applications as storage crystal luminophors for X-ray imaging [2, 4] and thermal neutron detection [5]. It should be noted that the neutron sensitivity (S_n) of $SrBPO_5:Eu^{2+}$ powder luminophors was found to be two orders of magnitude lower than that of the commercial $BaFBr:Eu^{2+}$–Gd_2O_3 material [5]. Nevertheless, $SrBPO_5:Eu^{2+}$ solid solutions have been presented as possible candidates for a new nuclear imaging plate, since the low S_γ/S_n ratio (~$2\cdot10^{-3}$) of these luminophors is favorable for reducing the gamma-ray influence on the signal in the case when both neutrons and γ-radiation take place. This fact inspired us to study alkaline earth borophosphates doped with other rare earth ions.

In this paper, we report the luminescence of Ce^{3+} ions in alkaline earth (Sr, Ba) borophosphates. The Ce^{3+} ion shows allowed $4f \leftrightarrow 5d$ transitions in absorption and emission. The emission band has usually a doublet structure which is due to the spin orbit spitting of the $4f^1$ ground state into two components $^2F_{5/2}$ and $^2F_{7/2}$ with a separation of about 2000 cm^{-1}. Since the decay time of Ce^{3+} emission in a crystal is shorter than that of Eu^{2+} emission (typically 20–70 ns vs. ~0.8 μs), a screen containing

Ce^{3+}-doped luminophor can be read faster, enabling high-speed imaging. The luminescence properties of Ce^{3+} in $CaBPO_5$ have been reported recently [6]. It was found that the Ce^{3+} ion in $CaBPO_5$ shows an efficient $5d \rightarrow 4f$ luminescence with maxima at 320 and 340 nm. The decay time of this emission is short (19.5 ns). This paper is focused on the effect of alkaline earth ion on the electronic structure and the luminescence properties of $MBPO_5$ (M = Sr, Ba) doped with Ce^{3+} ions.

It is widely accepted [2–4, 7] that the crystal structure of $MBPO_5$ does not differ significantly from that of mineral stillwellite $CeBO(SiO_4)$ described in detail in [8]. The assumption of crystal similarity with stillwellite is consistent with X-ray powder diffraction patterns of $MBPO_5$ (M = Ca, Sr, Ba) [1, 7]. In the crystal structure of $CeBO(SiO_4)$, each BO_4 group is connected with two SiO_4 groups and has two common edges with cerium polyhedrons [8]. The Ce^{3+} ions are surrounded by nine oxygen ions. It is important to note that in the stillwellite structure, the anions of different nature (SiO_4 and BO_4) are connected with each other. This is the most prominent structural feature of stillwellite (and alkaline earth borophosphates $MBPO_5$, too), because in compounds with mixed oxide anions, the anion groups of various nature are usually isolated [9].

The $M_{1-x-y}Ce_xNa_yBPO_5$ ($x = y = 0.01$) solid solutions were prepared using solid state reactions. The starting mixtures of MCO_3, BPO_4, $Ce(NO_3)_3 \cdot 6H_2O$, and Na_2HPO_4 were calcined at a temperature of about 300°C for 1 h, 600°C for 3 h, and then at 850°C for 8 h in air. The samples were cooled, mortared to insure homogeneity and calcined again at 850°C for 8 h in a reducing atmosphere (CO). The starting powders were co-doped with alkali ions (Na^+), because Na^+ on an alkaline earth site acts as a charge compensating defect for Ce^{3+}. All samples were examined by X-ray diffraction (XRD) using Cu K_α radiation. No impurity phases were detected in the XRD patterns. The emission and excitation spectra were recorded at room temperature using a LOMO SDL 1 spectrofluorimeter equipped with a xenon lamp. The spectra were corrected for the photomultiplier sensitivity and the monochromator efficiency using a calibrated light source. For the decay time measurements, a pulsed YAG:Nd^{3+} laser ($\lambda_{exc} = 266$ nm) was employed. The measurements of excitation spectra at wavelengths shorter than 230 nm and the decay time measurements were performed at 8 K and room temperature using synchrotron radiation and the equipment of the SUPERLUMI experimental station [10] of HASYLAB (Hamburg, Germany). The vacuum ultraviolet (VUV) excitation spectra were corrected for the wavelength dependent excitation intensity with the use of sodium salicylate as a standard. The ultimate spectral resolution was about 1 nm. X-ray induced emission spectra were recorded using an X-ray tube with a Cu anode operated at 35 kV and 25 mA. For thermally stimulated luminescence measurements (TSL), a $^{90}Sr/^{90}Y$ β-source installed in a Ris∅TL/OSL-DA 15 A/B reader was applied. The dose rate was 1.0 mGy/s in air.

The emission spectra of Ce^{3+} ions in $BaBPO_5$ and $SrBPO_5$ exhibit nearly the same characteristics. The spectra consist of two overlapping bands with maxima at about 319 and 339 nm which are ascribed to transitions from the lowest Ce^{3+} $5d$ excited state to the $4f$ ground state levels $^2F_{5/2}$ and $^2F_{7/2}$. The energy gap between the maxima coincides with the spin-orbit splitting of Ce^{3+} ground state, which amounts to about 2000 cm^{-1}. Fig. 1 shows the time-resolved VUV excitation spectra for $Sr_{1-x-y}Ce_xNa_y$-BPO_5 ($x = y = 0.01$) at 8 K. The short-time excitation spectrum consists of the bands at 192, 219 241, 258, and 277 nm. It is obvious that these bands are due to direct excitation of the Ce^{3+} ions via transitions to the components of the Ce^{3+} $5d$ configuration. Also, there is a strong band with a maximum at about 8.21 eV (151 nm). The time-integrated excitation spectrum has the same structure. In addition to the $4f$–$5d$ excitation bands, there is a sharp increase of the emission intensity between 7.2 and 8.2 eV. The local maximum at 8.21 eV can be assigned to a band gap transition with a subsequent energy transfer to the Ce^{3+} ions. Probably, a valley at about 8.75 eV is caused by a small penetration depth of the excitation radiation in this region resulting in the luminescence quenching. Beyond the valley, the emission intensity increases steadily with increasing excitation energy. It is important to note that in the 7–15 eV region, the excitation spectrum is very similar to those for $CaBPO_5$ doped with either Ce^{3+} [6] or Eu^{3+} [3].

The emission decay curves of $Sr_{1-x-y}Ce_xNa_yBPO_5$ ($x = y = 0.01$) at 8 K for three different excitation wavelengths are presented in Fig. 2.

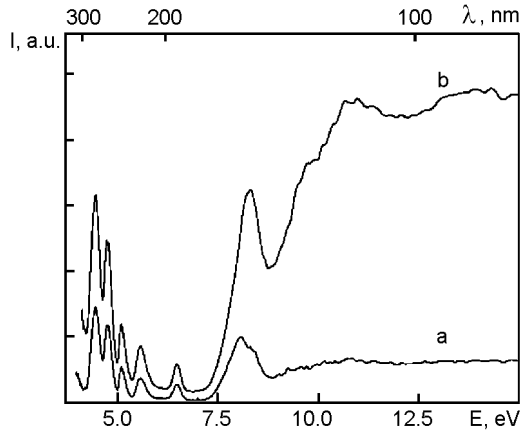

Fig. 1. Time-resolved excitation spectra of $Sr_{1-x-y}Ce_xNa_yBPO_5$ ($x = y = 0.01$) monitoring the $5d \rightarrow 4f$ emission of Ce^{3+} ($\lambda_{em} = 320$ nm) at 8 K. The spectra were recorded for two different time intervals after picosecond pulse excitation; between 1.5 and 7.5 ns (a), between 1.5 and 200 ns (b).

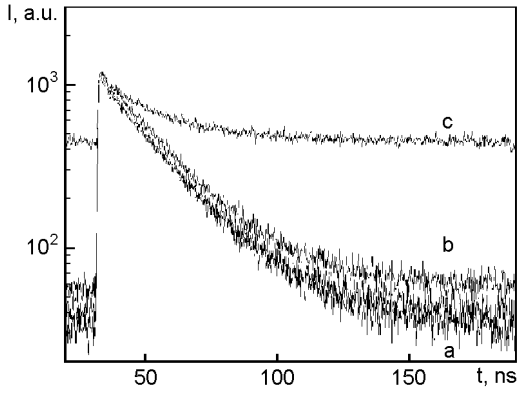

Fig. 2. 320 nm emission decay curves for $Sr_{1-x-y}Ce_xNa_yBPO_5$ ($x = y = 0.01$) recorded upon excitation at 266 nm (a), 150 nm (b), and 82.7 nm (c). Measurements were performed at 8 K.

Upon excitation at $\lambda_{exc} = 266$ nm, the decay is nearly exponential and its initial stage can be characterized by the time constant (τ) of 20.5±1 ns. Upon excitation at $\lambda_{exc} = 150$ nm (8.27 eV), the decay (Fig. 2, curve b) shows practically the same behavior. This indicates that the energy transfer from the excitons to Ce^{3+} ions is fast and efficient. Under excitation in the 9–15 eV region, a slow component with a $\tau \approx 10^{-6}$ s appears in the decay. This indicates that the excitation of cerium ions is caused by sequential hole and electron captures. Since the synchrotron operated in multi-bunch mode with bunches separated by 200 ns, the decay curve for $\lambda_{exc} = 82.67$ nm (15 eV) reflects the accumulative action of several exciting pulses. Note that upon heating the sample to room temperature, a contribution of slow component to the total signal significantly decreases.

As mentioned above, the emission spectrum of Ce^{3+} in $BaBPO_5$ consists of two bands with maxima at about 319 and 339 nm. The decay time of this emission upon UV excitation was found to be ~20 ns. The time-resolved VUV excitation spectra for $Ba_{1-x-y}Ce_xNa_yBPO_5$ ($x = y = 0.01$) at 8 K are shown in Fig. 3. It is evident that the excitation bands at 195, 215, 237, 260 and 276 nm are due to direct excitation of Ce^{3+} ions via transitions to the crystal-field components of the Ce^{3+} $5d$ configuration. Also, there is an excitation band with an edge at 7.15 eV (173 nm) and a maximum at 8.05 eV (154 nm), which can be attributed to the host lattice absorption. In the 8.1–8.5 eV region, the emission intensity drops rapidly. Between 9.5 and 15 eV, the emission intensity increases steadily with increasing excitation energy.

After exposure of the $MBPO_5:Ce^{3+}$ solid solutions to β radiation, a TSL signal is observed. In Fig. 4, TSL glow curves of the $Sr_{1-x-y}Ce_xNa_yBPO_5$ ($x = y = 0.01$) and $Sr_{2(1-x)}Ce_{2x}B_5O_9Br$ ($x = 0.01$) samples after β irradiation for 20 s at room temperature are compared. Note that the TSL spectrum of $Sr_{1-x-y}Ce_xNa_yBPO_5$ ($x = y = 0.01$) appears to be similar to the X-ray- or photoinduced emission spectra, indicating that the TSL originates from Ce^{3+}-related centers. The TSL glow curve of $Sr_{1-x-y}Ce_xNa_yBPO_5$ ($x = y = 0.01$) consists of a stronger peak at about 445 K and a weaker one with a maximum at about 385 K. As it is seen from Fig. 4, the TSL output from $SrBPO_5:Ce^{3+}$ is more than one order of magnitude lower as compared to the $Sr_2B_5O_9Br:Ce^{3+}$ luminophor, while both strontium borophosphate and strontium haloborate doped with Ce^{3+} exhibit a very intense X-ray induced emission of comparable magnitudes. The observed difference in the TSL output of $SrBPO_5:Ce^{3+}$ and $Sr_2B_5O_9Br:Ce^{3+}$ can be explained by the different origin of defects responsible for the TSL. The TSL glow curve of $Sr_2B_5O_9Br:Ce^{3+}$ consists of two peaks at about 350 and 430 K (Fig. 4). It has been shown recently that the stronger peak at 430 K can be attributed to the defects related to the bromine ion or its vacancy [11, 12]. It is obvious that such defects are absent in $SrBPO_5:Ce^{3+}$. At this

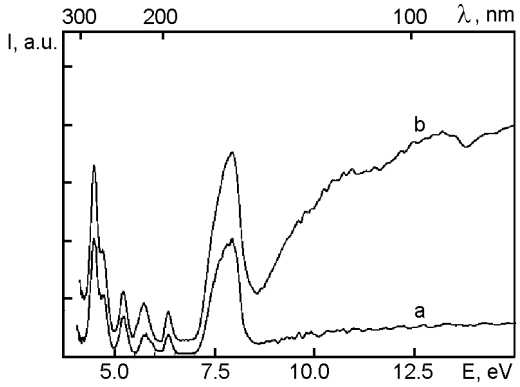

Fig. 3. Time-resolved excitation spectra of $Ba_{1-x-y}Ce_xNa_yBPO_5$ ($x = y = 0.01$) monitoring the $5d \rightarrow 4f$ emission of Ce^{3+}(λ_{em} = 320 nm) at 8 K. The spectra were recorded for two different time intervals after picosecond pulse excitation; between 1.5 and 7.5 ns (a), between 1.5 and 200 ns (b).

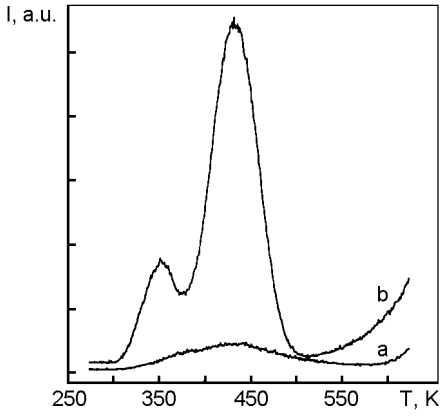

Fig. 4. TSL glow curves of β-irradiated (a) $Sr_{1-x-y}Ce_xNa_yBPO_5$ ($x = y = 0.01$) and (b) $Sr_{2(1-x)}Ce_{2x}B_5O_9Br$ ($x = 0.01$) for the integrated emission. The heating rate is 1 K/s.

stage, we can only speculate about the origin of trapping levels in $SrBPO_5:Ce^{3+}$. The most probable candidates are defects in the borophosphate sublattice such as oxygen vacancies, as was proposed before for other oxide systems [13, 14].

In the Table, the luminescence characteristics of the doubly doped $MBPO_5:Ce^{3+}$, M^* (M = Sr, Ba; M^* = Na) samples are compared. The literature data on $CaBPO_5:Ce^{3+}$, Na^+ [6] and $Sr_2B_5O_9X:Ce^{3+}$ (X = Cl, Br) [11, 15] are added. Recently, it has been shown that the depression in energy position of the lowest $5d$ level of Ce^{3+} ion in a crystal can be considered as a result of two independent contributions, namely the centroid shift ε_c, defined as the energy shift of the barycenter of the Ce^{3+} $5d$ configuration relative to the free ion value (51225 cm^{-1}), and the total crystal field splitting ε_{cfs}, defined as the energy difference between the maxima of the highest and lowest $4f \rightarrow 5d$ bands in the excitation spectra [16, 17]. The magnitude of centroid shift ε_c depends mainly on the covalency of the Ce^{3+}-ligand bond and the polarizability of the ligands coordinating Ce^{3+}. Crystal field splitting is determined by the size and shape of the coordination polyhedron around Ce^{3+} [16–18]. From the Table, it is seen that with increasing size of the cation (R) of the host lattice, the lowest excitation band shifts to higher energies, the total crystal field splitting ε_{cfs} decreases. It should be noted that the crystal field splitting of the Ce^{3+} $5d$ configuration in $MBPO_5$ is relatively large for ninefold coordination. For example, ε_{cfs} for Ce^{3+} ions in $Sr_2B_5O_9X$ (X = Cl, Br) was found to be ~13200 cm^{-1} [11, 15]. Also, ε_{cfs} for Ce^{3+} ions in SrB_4O_7 is 12600 cm^{-1} [19]. The conclusion that the crystal field splitting of the Ce^{3+} $5d$ configuration in $MBPO_5$ is relatively large coincides with the results of high-frequency EPR study of $SrBPO_5:Eu^{2+}$ powder materials [4]. The Eu^{2+} ion in $SrBPO_5$ has been shown to occupy the Sr site and the $5d$ state undergoes considerable crystal field splitting due to a strong axial field.

Table. Comparison of the luminescent properties of Ce^{3+} ions in $MBPO_5:Ce^{3+}$, M^* (M^* = Na)

Compound	$R(M)$, Å	Crystal field splitting (ε_{cfs}), cm^{-1}	Centroid shift (ε_c), cm^{-1}	Stokes shift (σ), cm^{-1}
$CaBPO_5$	1.04	16600	8240	3520
$SrBPO_5$	1.17	15980	8405	4750
$Sr_2B_5O_9Cl$	1.17	13200	12470	1220
$Sr_2B_5O_9Br$	1.17	13100	13070	1170
$BaBPO_5$	1.38	15050	8290	4950

It is interesting to note that the observed values of ε_c for $MBPO_5:Ce^{3+}$ are between the typical values for phosphates (7000–8000 cm^{-1}) and borates (~9000 cm^{-1}) with a high degree of condensation of the anion groups [17, 18]. This agrees with the observation that the electronegativity of the PO_4 group is higher than that of the BO_4 group [20]. The centroid shift ε_c for $MBPO_5:Ce^{3+}$ (M = Ca, Sr, Ba) is expected to decrease with increasing M–O distance, however, ε_c was estimated to be practically the same. This is probably due to differences in details of the Ce^{3+} site distribution in $MBPO_5$ (M = Ca, Sr, Ba).

In the sequence Ca → Sr → Ba, the Stokes shift (δ) of the Ce^{3+} emission in $MBPO_5$ increases. It is well known that when Ce^{3+} ion is incorporated in a lattice on a larger cationic site, the relaxation in the excited state is larger and, therefore, the Stokes shift is larger. The Stokes shift of the Ce^{3+} emission in $SrBPO_5$ is quite large as compared with those of strontium haloborates (see Table). This observation indicates a strong relaxation of Ce^{3+} ion in the 5*d* excited state.

The strong resemblance between the VUV excitation spectra for $MBPO_5:Ce^{3+}$ (Figs. 1, 2) points to a similar origin of their fundamental absorption bands. This implies that the fundamental absorption band of the alkaline earth borophosphates is not related to the *p*-states of the alkaline earth ions, but is due to transitions within the anion sublattice. In other words, the top of $MBPO_5$ valence band arises from 2*p* oxygen states. Transitions from these states to vacant 3*s* and 3*p* phosphorus states (2*s*, 2*p* boron states) cause the dominant features of the VUV excitation spectrum. The authors [21] have reported the energy levels scheme of the tetrahedral PO_4^{3-} group. The lowest intramolecular transition O $2p \rightarrow$ P 3*s* is expected to occur at 8.6 eV. Later, the electronic structure of the $B_3O_9^{9-}$ anionic group in which three BO_4 tetrahedrons are linked to each other was calculated [22]. The lowest O $2p \rightarrow$ B 2*s*, 2*p* transition is estimated to occur at about 8.4 eV. On the other hand, depending on the type of borate group, the band gap energy of alkaline earth borates varies between 6.3 and 8 eV, so that from the measurements presented, it cannot be determined which of the states (P or B) are involved in the fundamental absorption. Also, taking into account the presence of B–O–P bonds in $MBPO_5$, it cannot be excluded that the states near the bottom of conduction band have a complex, mixed character.

In conclusion, the short decay time (~20 ns) of the Ce^{3+} emission upon $4f \rightarrow 5d$ excitation provides a possibility for fast photostimulated luminescence of $MBPO_5:Ce^{3+}$ materials. Taking into account the favorable chemical composition and luminescence characteristics, the $MBPO_5:Ce^{3+}$ solid solutions may be of value for application in thermal neutron dosimetry. The study of the storage properties of these materials is in progress.

References

1. G.Blasse, A.Bril, J.De Vries, *J. Inorg. Nucl. Chem.*, **31**, 568 (1969).
2. A.Karthikeyani, R.Jagannatan, *J. Luminescence*, **86**, 79 (2000).
3. Q.Su, H.Liang, T.Hu et al., *J. Alloys Comp.*, **344**, 132 (2002).
4. T.Nakamura, T.Takeyama, N.Takahashi et al., *J. Luminescence*, **102–103**, 369 (2003).
5. K.Sakasai, M.Katagiri, K.Toh et al., *J. Appl. Phys.*, **A 74**, S1589 (2002).
6. P.Dorenbos, L.Pierron, L.Dinca et al., *J. Phys.:Condens. Matter.*, **15**, 511 (2003).
7. A.M.Srivastava, *J. Luminescence*, **78**, 239 (1998).
8. A.A.Voronkov, Yu.A.Pyatenko, *Kristallografiya*, **12**, 258 (1967).
9. B.F.Dzhurinsky, G.V.Lysanova, *Zh. Neorg. Khim.*, **43**, 2065 (1998).
10. G.Zimmerer, *Nucl. Instr. Meth.*, **A 308**, 178 (1991).
11. A.V.Sidorenko, A.J.J.Bos, P.Dorenbos et al., *J. Phys.:Condens. Matter.*, **15**, 3471 (2003).
12. A.V.Sidorenko, A.J.J.Bos, P.Dorenbos et al., *J. Phys.:Condens. Matter.*, **16**, 4131 (2004).
13. A.Meijerink, G.Blasse, M.Glasbeek, *J. Phys. D:Condens. Matter.*, **2**, 6303 (1990).
14. M.J.Knitel, P.Dorenbos, C.M.Combes et al., *J. Luminescence*, **69**, 32 (1996).
15. V.P.Dotsenko, I.V.Berezovskaya, N.P.Efryushina et al., *J. Luminescence*, **93**, 137 (2001).
16. P.Dorenbos, *Phys. Rev.*, **B 62**, 15650 (2000).
17. P.Dorenbos, *Phys. Rev.*, **B 64**, 125117/1-12 (2001).
18. P.Dorenbos, *Phys. Rev.*, **B 65**, 235110/1-6 (2002).
19. J.W.M.Verwey, G.J.Dirksen, G.Blasse, *J. Phys. Chem. Solids*, **53**, 367 (1992).
20. V.P.Dotsenko, M.G.Zuev, S.V.Ermakova, T.Z.Seyfullina, *Zh. Fiz. Khim.*, **63**, 2106 (1989).
21. V.A.Gubanov, A.L.Ivanovsky, M.V.Ryzhkov, Quantum Chemistry in Materials Science, Nauka, Moscow (1987) [in Russian].
22. M.V.Ryzhkov, V.P.Dotsenko, N.P.Efryushina, V.A.Gubanov, *Zh. Strukt. Khim.*, **32**, 26 (1991).

Люмінесцентні властивості іонів Ce^{3+} у лужноземельних борофосфатах

В.П.Доценко, І.В.Березовська, Н.П.Єфрюшина, А.С.Волошиновський, К.ван Ейк, П.Доренбос, А.В.Сидоренко

Досліджено люмінесцентні властивості іонів Ce^{3+} у лужноземельних борофосфатах $MBPO_5$ (M = Sr, Ba) в області 3.5–15 еВ. Показано, що розщеплення $5d$-конфігурації іона Ce^{3+} в $MBPO_5$ (M = Sr, Ba) кристалічним полем відносно велике, проте, нижчий $5d$-стан іонів Ce^{3+} характеризується досить великою енергією, що обумовлено високим ступенем іонності зв'язку M–O. Зіставлення спектрів збудження люмінесценції показує, що смуга фундаментального поглинання $MBPO_5$ обумовлена переходами в аніонних групах.